Human Pathology (2019) **91**, 19–25

ELSEVIER

Human PATHOLOGY

www.elsevier.com/locate/humpath

Original contribution

Distinct histomorphological features are associated with *IDH1* mutation in intrahepatic cholangiocarcinoma

Tao Wang MD[a], Esther Drill PhD[b], Efsevia Vakiani MD, PhD[a], Linda Ma Pak MD[c], Thomas Boerner MD[c], Gokce Askan MD[a], Juan Manuel Schvartzman MD, PhD[d], Amber L. Simpson PhD[c], William R. Jarnagin MD[c], Carlie S. Sigel MD[a,*]

[a]*Department of Pathology, Memorial Sloan Kettering Cancer Center, New York, NY, 10065 USA*
[b]*Department of Biostatistics, Memorial Sloan Kettering Cancer Center, New York, NY, 10065 USA*
[c]*Department of Surgery, Memorial Sloan Kettering Cancer Center, New York, NY, 10065 USA*
[d]*Department of Medicine, Memorial Sloan Kettering Cancer Center, New York, NY, 10065 USA*

Received 27 March 2019; revised 6 May 2019; accepted 7 May 2019

Keywords:
Cholangiocarcinoma;
Histology;
Liver cancer;
Genomics;
IDH1

Summary Intrahepatic cholangiocarcinoma has known histological heterogeneity. Mutations in *IDH1* (m*IDH1*) define a molecular subclass of intrahepatic cholangiocarcinoma and *IDH*-targeted therapies are in development. Characterizing m*IDH1* ICC histomorphology is of clinical interest for efficient identification. Resected ICCs with targeted next-generation sequencing by MSK-IMPACT were selected. Clinical data were obtained. By slide review, blinded to *IDH* status, data were collected for histology type, mucin production, necrosis, fibrosis, cytoplasm cell shape (low cuboidal, plump cuboidal/polygonal, and columnar), and architectural pattern (anastomosing, tubular, compact tubular, and solid). A tumor was considered architecturally heterogeneous if no dominant pattern represented ≥75% of the tumor. Parameters were compared between m*IDH1*and *IDH* wild-type controls. In the examined cohort (113 ICC: 29 m*IDH1* and 84 *IDH* wild-type), all *IDH1*-mutant tumors were of small duct–type histology, thus analysis was limited to 101 small duct–type tumors. m*IDH1*cases were more likely to have plump cuboidal/polygonal shape (P = .014) and geographic-type fibrosis (P = .005), while *IDH1* wild-type were more likely to have low cuboidal shape (P = .005). Both groups were predominantly architecturally heterogeneous with no significant difference in the distribution of architectural patterns. Plump cuboidal/polygonal cell shape and a geographic-type pattern of intra-tumoral fibrosis are more often seen in m*IDH1*compared to *IDH* wild-type tumors; however, *IDH1* mutation is not associated with a distinct histoarchitectural pattern.

☆ Funding Disclosure and Conflict of Interest Statement: This work was funded in part by the Marie-Josée and Henry R. Kravis Center for Molecular Oncology, the Cancer Center Support Grant of the National Institutes of Health/National Cancer Institute [P30CA008748], and Cycle for Survival. Carlie Sigel received reimbursement for transportation to attend one meeting from Agios Pharmaceuticals. The content is solely the responsibility of the authors and does not necessarily represent the official views of the National Institutes of Health. The manuscript is not under consideration for publication elsewhere. Preliminary data was presented as a poster at USCAP 2018 in Vancouver, BC by Dr. Tao Wang. This manuscript has not been published in whole or in part elsewhere. We attest to the fact that all authors have read and approved the manuscript and agree to its submission to this journal.

* Corresponding author at: 1275 York Ave, New York, NY 10065.
E-mail address: sigelc@mskcc.org (C. S. Sigel).

https://doi.org/10.1016/j.humpath.2019.05.002
0046-8177/

1. Introduction

Biliary adenocarcinomas are classified as intrahepatic, peri-hilar and extrahepatic based on their anatomical location. Intrahepatic cholangiocarcinoma (ICC) is a rare tumor in western populations with an incidence of approximately 4 to 10 per 100 000 person years and a 5-year survival rate of around 15% [1]. Surgical resection with curative intent offers a 5-year survival of 20% to 40% [2].

Recent genomic studies have shown that neomorphic mutations in isocitrate dehydrogenase 1 (*IDH1*) in cholangiocarcinoma is highly associated with intrahepatic origin, with a prevalence of approximately 20% in North American studies [3,4]. IDH1 is an enzyme in the tricarboxylic acid cycle that catalyzes the oxidative decarboxylation of isocitrate to α-ketoglutarate. Neomorphic mutations in this enzyme, which also occur in acute myeloid leukemia, gliomas, and chondrosarcoma, typically lead to altered activity that results in the increased production of (R)-2-hydroxyglutarate, which interferes with histone and DNA demethylases, as well as several other α-ketoglutarate-consuming processes [5-8]. An additional consequence of this mutation in myeloid neoplasms and glioma is interference with tumor differentiation [9]. Mutations in *IDH1* tend to occur in hotspots such as R132, and in ICC the most common mutations are R132C, R132G, and R132L, which are distinct from the R132H mutation found in gliomas and not detected by commercially available immunohistochemical stains [5,10]. Nonetheless, these activating mutations have been shown to increase the serum level of (R)-2-hydroxyglutarate in cholangiocarcinoma [11]. In cholangiocarcinoma, the effects of interference with phenotypic or functional differentiation are of great interest.

Given the singular metabolic disruption of *IDH1*-mutated neoplasms, it is logical to consider whether this

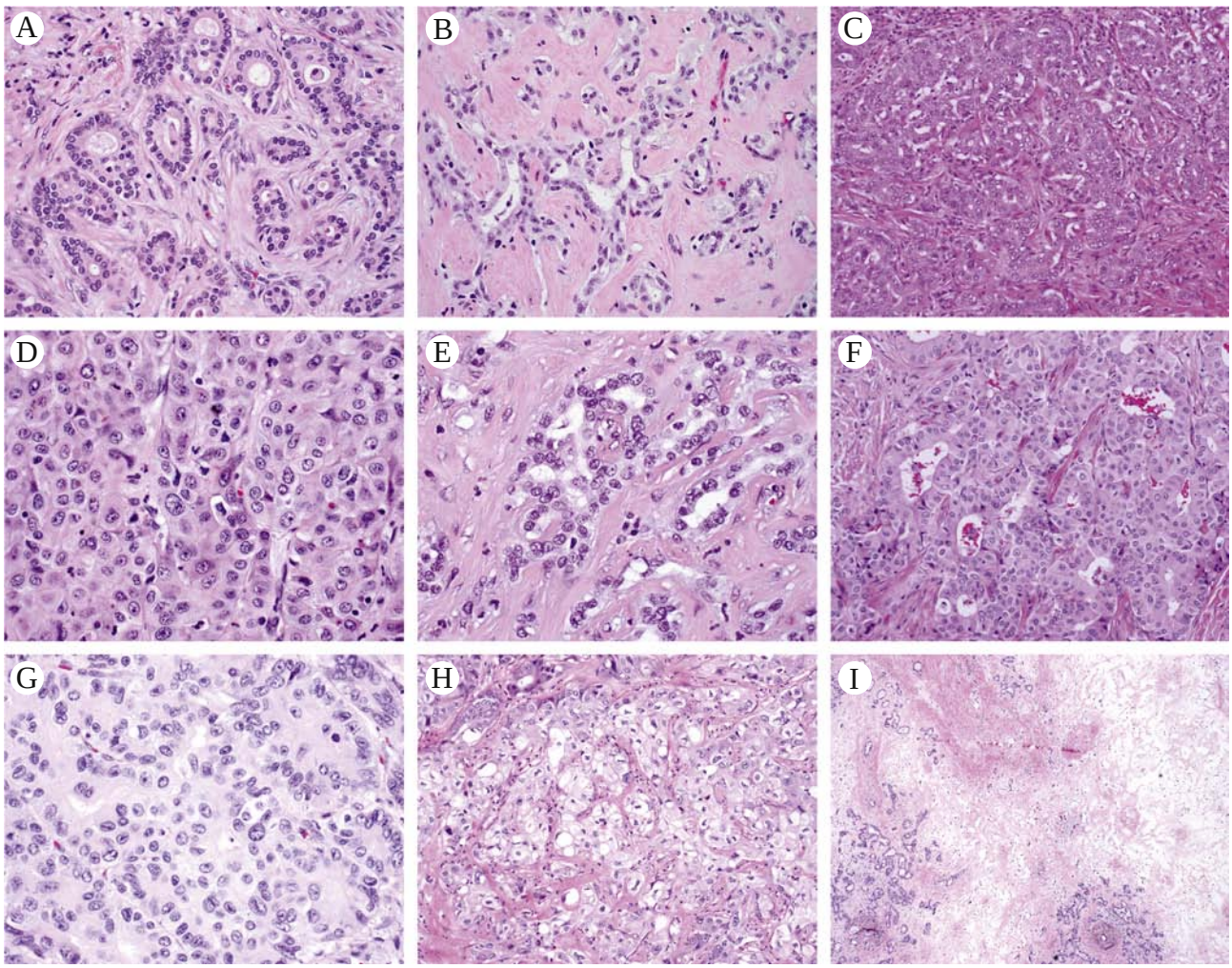

Fig. 1 The various architectural patterns and cell shapes evaluated in this study are illustrated using *IDH1* mutant intrahepatic cholangiocarcinomas. A, Simple tubular pattern ;. B, Anastomosing pattern ;. C, Compact tubular pattern ;. D, Solid pattern ;. E, Low cuboidal shape ;. F and G, Plump cuboidal shapes line lumens, and polygonal cells are seen in crowded or solid areas ;. H, Clear cell features ;. I, Geographic fibrosis.

Table 1 Clinical characteristics of patients with *IDH1*-mutant and *IDH* wild-type intrahepatic cholangiocarcinoma, small duct type

Variable	Wild-type *IDH*	Mutant *IDH1*	*P*
	N = 72	N = 29	
Age (median, IQR)	67 (58, 73)	73 (65, 78)	.052
Sex			.7
F	42 (58%)	15 (52%)	
M	30 (42%)	14 (48%)	
Ethnicity			.3
Asian	6 (8.3%)	2 (6.9%)	
Black	6 (8.3%)	0 (0%)	
White	60 (83%)	27 (93%)	
Autoimmune disease	3 (4.2%)	6 (21%)	.016
Chronic viral hepatitis B/C	9 (19%)	3 (14%)	.7
Unknown	25	8	
Smoking	29 (40%)	14 (50%)	.5
Unknown	0	1	
Clinical cirrhosis	7 (9.7%)	1 (3.6%)	.4
Unknown	0	1	
Frequent alcohol	3 (4.2%)	3 (11%)	.3
Unknown	0	1	
Steatosis	4 (5.6%)	3 (11%)	.4
Unknown	0	2	
Neoadjuvant chemotherapy (systemic or intrahepatic)			>.9
Any chemo	7 (9.7%)	3 (11%)	
No chemo	65 (90%)	25 (89%)	
Unknown	0	1	

Table 2 Histopathological characteristics of *IDH1*-mutant and *IDH* wild-type intrahepatic cholangiocarcinoma, small duct type[a]

Variable	Wild-type *IDH*	Mutant *IDH1*	*P*
	N = 65	N = 25	
Median tumor size (cm, range)	6.0 (4.2, 8.4)	5.5 (3.8, 6.5)	.14
Unknown	2	0	
Heterogeneous histology	44 (68%)	18 (72%)	.9
Homogeneous: anastomosing	6 (9.2%)	0	.2
Homogeneous: compact tubular	11 (17%)	4 (16%)	>.9
Homogeneous: solid	2 (3.1%)	2 (8.0%)	.3
Homogeneous: simple tubular	2 (3.1%)	1 (4.0%)	>.9
% Anastomosing (median, range)	15 (0,35)	18 (5,40)	.7
% Tubular (median, range)	0 (0,20)	10 (0,20)	.10
% Compact (median, range)	40 (25,70)	35 (23,64)	.5
% Solid (median, range)	10 (0,30)	8(0,26)	.4
Necrosis (mean % volume)	3 (0, 0)	2 (0,11)	.6
Necrosis >25%	7 (11%)	0	.2
Necrosis (any)	39 (60%)	14 (56%)	>.9
Fibrosis (mean % volume)	14 (10, 20)	20 (15, 26)	.009
Geographic-type fibrosis	9 (14%)	11 (44%)	.005
Low cuboidal cell shape	58 (89%)	15 (60%)	.005
Plump cuboidal/polygonal shape	19 (29%)	15 (60%)	.014
Columnar cell shape	2 (3.1%)	0	>.9
Variable cytoplasm pattern	19 (29%)	8 (32%)	>.9
Intracellular mucin	8 (12%)	1 (4.0%)	.4
Extracellular mucin	17 (26%)	2 (8.0%)	.11
Clear cell features	24 (37%)	15 (60%)	.082
Grade			.8
1	32 (49%)	14 (56%)	
2	24 (37%)	9 (36%)	
3	9 (14%)	2 (8.0%)	
Perineural invasion	15 (24%)	7 (30%)	.8
Unknown	3	2	
Lymphovascular invasion	16 (25%)	4 (16%)	.6
Periductal infiltration	6 (9.2%)	2 (8.0%)	>.9
Satellite nodules	16 (25%)	4 (16%)	.6
AJCC 8th ed. primary tumor stage			.5
1	24 (37%)	13 (54%)	
2	32 (49%)	10 (42%)	
3	8 (12%)	1 (4.2%)	
4	1 (1.5%)	0 (0%)	
Unknown	0	1	
Regional lymph nodes (at resection)			.4
pN0	22 (34%)	5 (20%)	
pNx	8 (12%)	5 (20%)	
pN1	35 (54%)	15 (60%)	

[a] Tumors with neoadjuvant chemotherapy were excluded.

molecular subtype produces a recognizable phenotype. Intrahepatic cholangiocarcinoma has been subclassified by both gross and histological configuration with varying acceptance. Grossly, ICC occurs in mass forming, periductal infiltrating, and intraductal subtypes [12]. Histologic subtyping has gained less widespread acceptance and clinical significance is less substantiated. On the one hand, the neoplasms have been separated into "peripheral" and "hilar" subtypes [13,14]. Alternatively, the neoplasms have been divided into groups based on resemblance to large bile duct cells (large duct) versus cholangiolar cells (small duct type) [15]. Additional patterns such as ductal plate malformation have been described [16].

While the prognostic relevance of *IDH1* mutation is uncertain, it is expected to be of therapeutic relevance. Survival analysis of *IDH*-mutant ICC have shown conflicting results and are often limited in power because the mutation is present only in a subset of the populations studied [3,5,10,17,18]. Nonetheless, mutant *IDH1* represents a promising actionable target for small molecule therapy in leukemia, glioma, and cholangiocarcinoma and clinical trials are in progress [19-21]. This study aims to comprehensively evaluate the cytological and architectural features of *IDH1* mutated (m*IDH1*) ICC in comparison to ICC lacking hotspot mutations in *IDH1* and

IDH2 which could aid in the identification of *IDH1*-mutant tumors.

2. Materials and methods

This study was approved by the Institutional Research Ethics Board of Memorial Sloan Kettering Cancer Center. Surgically resected ICCs from 1993 to 2017 which had undergone targeted next-generation sequencing by MSK-IMPACT either on a clinical basis or as a part of retrospective, investigational testing (based on the availability of archived tumor and normal control tissue availability). MSK-IMPACT was clinically validated for the detection of mutations of *IDH1* exon 4 (41–138) and *IDH2* exon 4 (125–178) inclusive of hotspot mutations observed in intrahepatic cholangiocarcinoma [22]. Cases were stratified by the mutation status of *IDH1*. Tumors with *IDH2* mutations were excluded, therefore the wild-type *IDH* (wt*IDH*) was defined by lacking alterations in *IDH1* and *IDH2* as detected by MSK-IMPACT. The frequency of alterations was grouped by signaling pathways as determined using the Reactome open-source pathway database.

2.1. Clinical and pathologic variables

Clinical data including age at diagnosis, sex, ethnicity, history of autoimmune disease, chronic viral hepatitis, smoking, and clinical cirrhosis were obtained by review of electronic medical records. Pathology slides and reports were reviewed to assess characteristics of tumor size, grade, presence of perineural invasion, lymphovascular invasion, periductal infiltration, satellite nodules, presence of mucin, and intraductal precursor lesions. Small duct versus large duct types, results of albumin mRNA in situ hybridization, Arginase-1, and

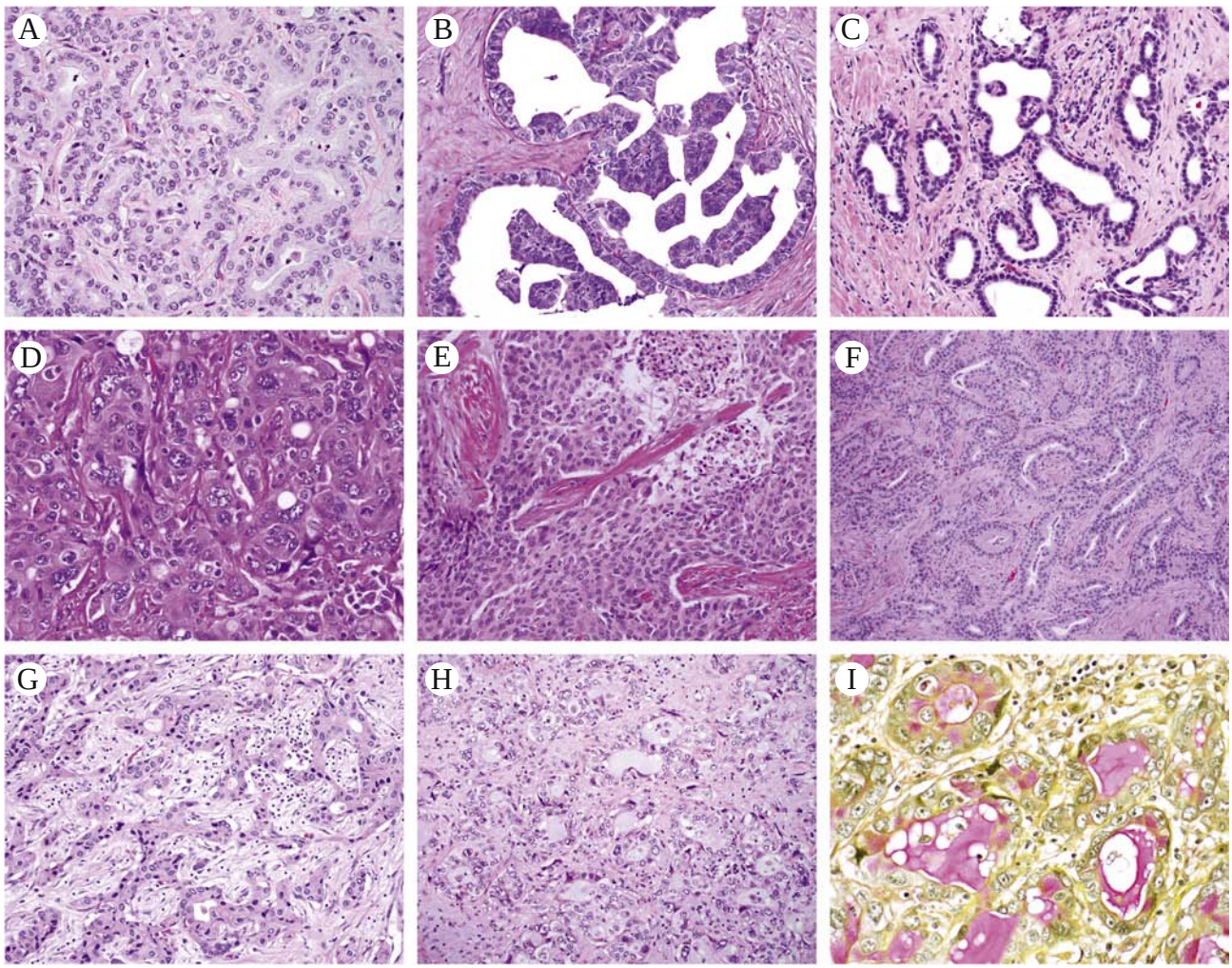

Fig. 2 A-I, Diverse histology and cell shape patterns are seen in *IDH1* mutants ;. A, Anastomosing glands with plump cuboidal cells ;. B, Micropapillary ;. C, Low cuboidal cells with dilated tubules ;. D, Pleomorphic nuclei in polygonal cells, solid pattern ;. E, Solid pattern ;. F, Tubular and anastomosing glands, plump cuboidal ;. G, Anastomosing glands plump cuboidal ;. H and I, Tubular pattern with cuboidal cells and focal intra- and extracellular mucin as highlighted by uciarmin stain in I.

Table 3 Mutations and genetic pathways in IDH1-mutant and IDH1 wild-type small duct intrahepatic cholangiocarcinoma

Variable	Wild-type *IDH*	Mutant *IDH1*	*P*
	N = 72	N = 29	
Gene			
ARID1A	18 (25%)	6 (21%)	.8
BAP1	11 (15%)	7 (25%)	.3
FGFR2	13 (18%)	0 (0%)	.017
KRAS	7 (9.7%)	0 (0%)	.2
PBRM1	14 (19%)	4 (14%)	.8
TP53	11 (15%)	5 (18%)	.8
Pathway			
SWI/SNF[a]	32 (44%)	9 (31%)	.3
DNA damage[b]	27 (38%)	14 (48%)	.4
MAPK[c]	29 (40%)	4 (14%)	.011
PI3K[d]	2 (2.8%)	3 (10%)	.14

[a] SWI/SNF: *ARID1A, PBRM1, ATRX.*
[b] DNA Damage: *BAP1, TP53, ATM, BRCA1, BARD1, KMT2A, KMT2C.*
[c] MAPK: *KRAS, FGFR2, NF1, ARAF, BRAF, RASA1, MAP2K1, MAPK3, PDGFRA, GRIN2A.*
[d] PI3K: *PTEN, PIK3R2, RPTOR.*

HepPar-1 immunohistochemistry were determined using methods and criteria from a prior publication [15]. Tumor grading was performed by applying the Bloom-Richardson system commonly used in breast carcinoma [23]. Clinical stage and lymph node status was assigned using the AJCC 8th edition using the available pathological and clinical information at the time of resection [24].

Tumor architecture was classified into 4 patterns as shown in Fig. 1A-D. The anastomosing pattern consisted of anastomosing small ductular structures like the ductular reaction. The simple tubular pattern consisted of non-anastomosing tubules with stroma between glands. The compact tubular pattern had lumens or slit-like spaces, but the glands were compressed together without intervening stroma. The solid pattern was confluent with minimal lumens. Architecturally heterogeneous comprised no one pattern ≥75% of the tumor across all reviewed slides. Percent of necrosis and fibrosis were evaluated by semi-quantitative estimation of volume involving tumor on each reviewed tumor slide with average across the aggregate of all tumor slides. Geographic-type fibrosis was defined as a discrete region of fibrosis without intervening viable tumor glands (Fig. 1I). The cell shape was categorized as low cuboidal, plump cuboidal/polygonal, and columnar as illustrated in Fig. 1. Low cuboidal had less than 1 nuclear diameter of apical cytoplasmic length, plump cuboidal/polygonal had between 1 and 2 nuclear diameters of apical cytoplasm or has cytoplasm which exceeds 2x the width of the nuclei, and columnar cells had more than 2 nuclear diameters of apical cytoplasm with or without mucin. Clear cell features were recorded as present if seen in >10% of tumor cells (Fig. 1H).

2.2. Statistical methods

Statistical comparisons were performed by Fisher's exact test for categorical variables. For histological comparisons, tumors that underwent neoadjuvant therapy were excluded from the analysis, and only small duct–type tumors were included. For sensitivity and specificity, we tested *IDH1* mutation predictions from logistic regression models against observed *IDH1* mutation and used *IDH1* mutation prevalence as the prediction threshold cut-off. We analyzed for associations between *IDH1* mutation status for clinical and histological characteristics for all tumors, and then repeated the analysis for small duct–type tumors only. Tumors with slides reviewed from recurrence were included in *IDH1* morphology analysis. Statistical significance for all comparisons was set as $P \leq .05$.

3. Results

We identified 29 m*IDH1* ICC and a control population of 84 wt*IDH* ICC. The somatic alterations in *IDH1* exon 4 consisted of p.R132C in n = 23 (79.3%), p.R132L in n = 3 (10.3%), and p.R132G in n = 3 (10.3%). All mIDH1 were of small duct–type whereas large duct (n = 9) and indeterminate types (n = 3) comprised a minority of the wt*IDH* group. Since large duct and indeterminate were exclusively in the wt*IDH* group, they were excluded from clinicopathological analysis. For the clinical variables, only autoimmune disease was significantly associated with m*IDH1* (Table 1). The 6 patients with autoimmune diseases in the m*IDH1* group had Hashimoto's thyroiditis (n = 2), rheumatoid arthritis (n = 2), scleroderma (n = 1), and Crohn's colitis (n = 1). Patients with small duct–type wt*IDH* small duct–type had primary sclerosing cholangitis (n = 1), Bell's palsy (n = 1), and multiple sclerosis (n = 1).

Significant differences in cell shape and fibrosis pattern were detected (Table 2). Plump cuboidal/polygonal shape and geographic fibrosis were significant associated with m*IDH1* while low cuboidal shape was significantly associated with wt*IDH1* while. The presence of plump cuboidal/polygonal shape had a sensitivity of 60% and specificity of 71% for identifying *IDH1* mutation. Geographic-type fibrosis had a sensitivity 44% and specificity of 86% for identifying *IDH1* mutation. The presence of both features (plump cuboidal/polygonal shape and geographic fibrosis) had a sensitivity of 72% and specificity of 60% for identifying *IDH1* mutation.

IDH mutation status was not associated with an architectural pattern (Table 2). Examples of *IDH1*-mutant histology are shown in Fig. 2. The compact tubular pattern was the most common dominant pattern for both groups (14%-15%). The volumes for the patterns were similar for both groups (Table 2).

Necrosis and fibrosis were limited in all untreated tumors. The identification of mucin, intra- or extracellular, did not distinguish m*IDH1* from wt*IDH,* but was notably present in both

groups, albeit in a very low percentage of tumors and generally focal (Fig. 2H-I).

Staining for albumin mRNA by in situ hybridization did not show a statistically significant difference in the groups. Of 26 m*IDH1* tested, 17 (65%) were albumin positive and of the 56 wt*IDH* tested, 47 (83%) were albumin positive (P = .084). The results for immunohistochemistry for markers of hepatocellular differentiation was: Arginase-1: positive in 0/23 tested m*IDH1*, 1/74 tested wt*IDH*; HepPar1: positive in 0/24 m*IDH1*, 1/74 tested wt*IDH*.

FGFR2 rearrangements, and the corresponding signaling pathway (MAPK), were the only 2 significant other genomic differences between the wt*IDH* and m*IDH1* groups (Table 3).

4. Discussion

IDH1 mutated intrahepatic cholangiocarcinoma has uniquely altered cellular biology known to affect cellular differentiation on a molecular level. Our study systematically classified the phenotype of a large cohort of ICC with prior targeted sequencing analysis and comparatively analyzed the histoarchitectural patterns of untreated tumors with the aim to detect phenotypic characteristics associated with this mutation. After our initial observation that all m*IDH1* ICC were small duct–type, subsequent analysis excluded large duct and indeterminate types in the wild-type group. By comparing m*IDH1* and wt*IDH* control groups, we determined that m*IDH1* tumors have a significantly higher proportion of cells with plump cuboidal/polygonal shape (60% versus 29%, P = .014) and geographic fibrosis (44% versus 14%, P = .005).

Prior comparisons between m*IDH1* and non–*IDH*-mutant ICC have described a higher proportion of clear cell change and lower proportion of poor differentiation in m*IDH* tumors [4,10]. We did not confirm these differences; however, our methodology differed from other studies, for instance we included small duct histology only. There is no criteria-based system for grading differentiation for ICC and we experimentally applied a system borrowed from breast cancer grading to allow contributions to grade from mitotic activity and architecture. If we consider that our assessment of dominant (>75%) solid architecture is a surrogate marker of poor differentiation based on architecture only, there is no detectable difference between the groups.

Since complexity of histoarchitecture is a component of most criteria of tumor differentiation at various anatomic sites, another aim of this study was to determine whether m*IDH1*-related altered cellular differentiation would have an observable histoarchitectural association. Examining this question is of considerable interest, because intrahepatic cholangiocarcinoma has distinctive architectural patterns and several investigators have attempted to subclassify them based on the premise that the patterns may have potential clinical or biological significance [25,26]. Recently, for example, the ductal plate malformation pattern was shown to have an association with *ARID1A* mutation [27]. We discovered that m*IDH1* and wt*IDH* ICCs are equally architecturally heterogeneous with a strikingly similar distribution of dominant architectural patterns. As noted, instead of an architectural difference, a distinctive cytomorphological appearance was recognized. We find it especially interesting that the plump cuboidal/polygonal morphology resemble oncocytes and hepatocytes given metabolic and gene expression changes in these neoplasms. *IDH1* mutants accumulate the metabolite (R)-2-hydroxyglutarate, show high expression of mitochondrial genes by integrative genomic analysis, and high mitochondrial DNA copy number [5]. Increased mitochondria are a feature of oncocytes, which typically have plump/polygonal shape [5]. In vitro models and mouse studies have also shown that mutant *IDH* blocks hepatocyte differentiation and *IDH*-mutant ICC express a liver progenitor cell gene signature [28].

Among the clinical variables we assessed, only autoimmune disease had a significant association with *IDH1* mutation status. Notably, none of the m*IDH1* patients had autoimmune diseases directly associated with biliary disease such as primary sclerosing cholangitis. Worldwide, there are regional differences in risk factors for cholangiocarcinoma and molecular subtypes have been shown to cluster with clinical factors such as liver fluke infection [29]. This study of ICC was performed in a population lacking liver fluke infection, hepatolithiasis, biliary cysts, and with a lower prevalence of chronic hepatitis (18%) compared to other published ICC cohorts [13,30].

A potentially confounding factor is the possibility of increased biologic heterogeneity in the wt*IDH* group. Removing the large duct and indeterminate types from our analysis was intended to mitigate biological heterogeneity within the wt*IDH* group because they are morphologically distinct from small duct type and there is some evidence that the large duct type has distinct biology and molecular associations [13]. We explored for potential genomic heterogeneity by comparing the mutation profiles of the 2 groups. Except for *FGFR2* rearrangements, we found no significant differences between the 2 groups in the proportions of the most common mutations in ICC. Analysis that compared the detected mutations by grouping into signaling pathway only showed a significant difference in the MAPK pathway that includes FGFR2 rearrangements.

In summary, our findings indicate that m*IDH1* intrahepatic cholangiocarcinoma are small duct type and have significant differences in cell shape (plump cuboidal/polygonal) and fibrosis (geographic) pattern compared to wt*IDH*. The tumor architectural patterns we studied do not distinguish m*IDH1* and wt*IDH1* intrahepatic cholangiocarcinoma.

Acknowledgements

We gratefully acknowledge the administrative support of Shanna Guercio, Sarah King, Marco Gonzalez, and Rebecca Andrade, laboratory support from Dr. Achim Jungbluth and

Denise Frosina, and members of the Molecular Diagnostics Service in the Department of Pathology.

References

[1] Flemming JA, Zhang-Salomons J, Nanji S, Booth CM. Increased incidence but improved median overall survival for biliary tract cancers diagnosed in Ontario from 1994 through 2012: a population-based study. Cancer 2016;122:2534-43https://doi.org/10.1002/cncr.30074.

[2] Meza-Junco J, Montano-Loza AJ, Ma M, Wong W, Sawyer MB, Bain VG. Cholangiocarcinoma: has there been any progress? Can J Gastroenterol 2010;24:52-7.

[3] Jiao Y, Pawlik TM, Anders RA, et al. Exome sequencing identifies frequent inactivating mutations in bap1, arid1a and pbrm1 in intrahepatic cholangiocarcinomas. Nat Genet 2013;45:1470-3https://doi.org/10.1038/ng.2813.

[4] Kipp BR, Voss JS, Kerr SE, et al. Isocitrate dehydrogenase 1 and 2 mutations in cholangiocarcinoma. Hum Pathol 2012;43:1552-8https://doi.org/10.1016/j.humpath.2011.12.007.

[5] Farshidfar F, Zheng S, Gingras MC, et al. Integrative genomic analysis of cholangiocarcinoma identifies distinct idh-mutant molecular profiles. Cell Rep 2017;19:2878-80https://doi.org/10.1016/j.celrep.2017.06.008.

[6] Fu X, Chin RM, Vergnes L, et al. 2-hydroxyglutarate inhibits atp synthase and mtor signaling. Cell Metab 2015;22:508-15https://doi.org/10.1016/j.cmet.2015.06.009.

[7] Parker SJ, Metallo CM. Metabolic consequences of oncogenic idh mutations. Pharmacol Ther 2015;152:54-62https://doi.org/10.1016/j.pharmthera.2015.05.003.

[8] Losman JA, Kaelin Jr WG. What a difference a hydroxyl makes: mutant idh, (r)-2-hydroxyglutarate. and cancer Genes Dev 2013;27:836-52https://doi.org/10.1101/gad.217406.113.

[9] Lu C, Ward PS, Kapoor GS, et al. Idh mutation impairs histone demethylation and results in a block to cell differentiation. Nature 2012;483:474-8https://doi.org/10.1038/nature10860.

[10] Goyal L, Govindan A, Sheth RA, et al. Prognosis and clinicopathologic features of patients with advanced stage isocitrate dehydrogenase (idh) mutant and idh wild-type intrahepatic cholangiocarcinoma. Oncologist 2015;20:1019-27https://doi.org/10.1634/theoncologist.2015-0210.

[11] Delahousse J, Verlingue L, Broutin S, et al. Circulating oncometabolite d-2-hydroxyglutarate enantiomer is a surrogate marker of isocitrate dehydrogenase-mutated intrahepatic cholangiocarcinomas. Eur J Cancer 2018;90:83-91https://doi.org/10.1016/j.ejca.2017.11.024.

[12] Aloia TPT, Taouli B, Rubbia-Brandt L, Vauthy J-N. Intrahepatic bile ducts. In: Amin MB, editor. Ajcc cancer staging manual, Chicago IL: American joint committee on Cancer, springer; 2017. p. 295-302.

[13] Aishima S, Kuroda Y, Nishihara Y, et al. Proposal of progression model for intrahepatic cholangiocarcinoma: Clinicopathologic differences between hilar type and peripheral type. Am J Surg Pathol 2007;31:1059-67https://doi.org/10.1097/PAS.0b013e31802b34b6.

[14] Nakanuma Y, Sato Y, Harada K, Sasaki M, Xu J, Ikeda H. Pathological classification of intrahepatic cholangiocarcinoma based on a new concept. World J Hepatol 2010;2:419-27https://doi.org/10.4254/wjh.v2.i12.419.

[15] Sigel CS, Drill E, Zhou Y, et al. Intrahepatic cholangiocarcinomas have histologically and immunophenotypically distinct small and large duct patterns. Am J Surg Pathol 2018;42:1334-45https://doi.org/10.1097/PAS.0000000000001118.

[16] Nakanuma Y, Sato Y, Ikeda H, et al. Intrahepatic cholangiocarcinoma with predominant "ductal plate malformation" pattern: a new subtype. Am J Surg Pathol 2012;36:1629-35https://doi.org/10.1097/PAS.0b013e31826e0249.

[17] Wang P, Dong Q, Zhang C, et al. Mutations in isocitrate dehydrogenase 1 and 2 occur frequently in intrahepatic cholangiocarcinomas and share hypermethylation targets with glioblastomas. Oncogene 2013;32:3091-100https://doi.org/10.1038/onc.2012.315.

[18] Zhu AX, Borger DR, Kim Y, et al. Genomic profiling of intrahepatic cholangiocarcinoma: refining prognosis and identifying therapeutic targets. Ann Surg Oncol 2014;21:3827-34https://doi.org/10.1245/s10434-014-3828-x.

[19] Fujiwara H, Tateishi K, Kato H, et al. Isocitrate dehydrogenase 1 mutation sensitizes intrahepatic cholangiocarcinoma to the bet inhibitor jq1. Cancer Sci 2018;109:3602-10https://doi.org/10.1111/cas.13784.

[20] Saha SK, Gordan JD, Kleinstiver BP, et al. Isocitrate dehydrogenase mutations confer dasatinib hypersensitivity and src dependence in intrahepatic cholangiocarcinoma. Cancer Discov 2016;6:727-39https://doi.org/10.1158/2159-8290.CD-15-1442.

[21] Dang L, Yen K, Attar EC. Idh mutations in cancer and progress toward development of targeted therapeutics. Ann Oncol 2016;27:599-608https://doi.org/10.1093/annonc/mdw013.

[22] Cheng DT, Mitchell TN, Zehir A, et al. Memorial Sloan Kettering-integrated mutation profiling of actionable cancer targets (msk-impact). A hybridization capture-based next-generation sequencing clinical assay for solid tumor molecular oncology J Mol Diagn 2015;17:251-64https://doi.org/10.1016/j.jmoldx.2014.12.006.

[23] Bloom HJ, Richardson WW. Histological grading and prognosis in breast cancer; a study of 1409 cases of which 359 have been followed for 15 years. Br J Cancer 1957;11:359-77.

[24] Amin MB, American Joint Committee on Cancer., American Cancer Society., Ajcc cancer staging manual, Eighth edition / editor-in-chief, Amin M ed., Chicago IL: American joint committee on Cancer, Springer, 2017.

[25] Nakanuma Y, Kakuda Y. Pathologic classification of cholangiocarcinoma: new concepts. Best Pract Res Clin Gastroenterol 2015;29:277-93https://doi.org/10.1016/j.bpg.2015.02.006.

[26] Sempoux C, Jibara G, Ward SC, et al. Intrahepatic cholangiocarcinoma: new insights in pathology. Semin Liver Dis 2011;31:49-60https://doi.org/10.1055/s-0031-1272839.

[27] Sasaki M, Sato Y, Nakanuma Y. Cholangiolocellular carcinoma with "ductal plate malformation" pattern may be characterized by arid1a genetic alterations. Am J Surg Pathol 2019;43:352-60https://doi.org/10.1097/PAS.0000000000001201.

[28] Saha SK, Parachoniak CA, Bardeesy N. Idh mutations in liver cell plasticity and biliary cancer. Cell Cycle 2014;13:3176-82https://doi.org/10.4161/15384101.2014.965054.

[29] Jusakul A, Cutcutache I, Yong CH, et al. Whole-genome and epigenomic landscapes of etiologically distinct subtypes of cholangiocarcinoma. Cancer Discov 2017;7:1116-35https://doi.org/10.1158/2159-8290.CD-17-0368.

[30] Yu TH, Yuan RH, Chen YL, Yang WC, Hsu HC, Jeng YM. Viral hepatitis is associated with intrahepatic cholangiocarcinoma with cholangiolar differentiation and n-cadherin expression. Mod Pathol 2011;24:810-9https://doi.org/10.1038/modpathol.2011.41.